APS physics

CHORUS

This is the accepted manuscript made available via CHORUS. The article has been published as:

Ergodicity breaking dynamics of arch collapse

Carl Merrigan, Sumit Kumar Birwa, Shubha Tewari, and Bulbul Chakraborty

Phys. Rev. E **97**, 040901 — Published 24 April 2018

DOI: 10.1103/PhysRevE.97.040901

Ergodicity breaking dynamics of arch collapse

Carl Merrigan,[1] Sumit Kumar Birwa,[2] Shubha Tewari,[3] and Bulbul Chakraborty[1]
[1] *Martin Fisher School of Physics, Brandeis University, Waltham MA, 02454**
[2] *TIFR International Center for Theoretical Sciences, Shivakote, Bengaluru 560089, India*
[3] *Department of Physics, University of Massachusetts, Amherst MA, 01003*
(Dated: April 9, 2018)

Flows in hoppers and silos are susceptible to clogging due to the formation of arches at the exit. The failure of these arches is the key to re-initiation of flow; yet the physical mechanism of failure is not well understood. Experiments on vibrated hoppers exhibit a broad distribution of the duration of clogs. Using numerical simulations of a hopper in two dimensions, we show that arches become trapped in locally stable shapes that are explored dynamically under vibrations. The shape dynamics, preceding failure, break ergodicity and can be modeled as a continuous time random walk (CTRW) with a broad distribution of waiting, or trapping times. We argue that arch failure occurs as a result of this random walk crossing a stability boundary, which is a first-passage process that naturally gives rise to a broad distribution of unclogging times.

Introduction Flows constrained by boundaries and driven towards an opening can arrest spontaneously due to the formation of an arch spanning the outlet [1, 2]. Understanding the physical properties of arches is thus crucial for preventing clogging of grains in silos or pedestrian traffic [1, 3–5]. The distribution of time intervals between clogging events is observed to be exponential [6–10]. In contrast, clog durations in vibrated silos [1, 2] or intermittent flows [11, 12], exhibit a broad distribution, which poses a challenge for devising efficient unclogging protocols. In this work, we identify the physical mechanism underlying the unclogging process as activated dynamics in a space of arch shapes. Using molecular dynamics simulations (MD) of a vibrated hopper (Fig. 1), we map out the dynamics of arches in a landscape of "shape" traps.

We observe a large variation in the stability of shapes (Fig. 2). The simplest mathematical representation of the dynamics is a *continuous* time random walk (CTRW) with a broad distribution of waiting times between steps, $\psi(t)$, which we determine through analysis of the arch dynamics. Such CTRWs are known to break ergodicity [13], and arise in trap models of glasses [14]. We demonstrate that the arch-dynamics indeed breaks ergodicity. The distribution of unclogging times is compatible with the distribution of times of "first passage"[15] of the CTRW to a boundary of stability in the space of arch shapes. Our numerical results are consistent with a recent analysis of unclogging experiments [16] using a trap model description of arch failure where the distribution of trap depths is broader than an exponential. To our knowledge, our simulations are the first to provide a detailed view of the dynamics of arch shapes leading up to the failure.

Numerical Simulations We perform MD simulations using LAMMPS [17] in a quasi two-dimensional (2D) hopper geometry (Fig 1). Analogous to experiments, where spherical grains are enclosed between two plates [1, 2], we constrain grains to move in the plane of the hopper. The grains interact via a Hertzian force law. The coefficient of static friction between the grains is $\mu_g = 0.8$. A 50 – 50 mixture of bidisperse spheres with diameter ratio 1 : 1.2 are randomly distributed inside the hopper, allowed to settle under gravity with the opening closed, then allowed to flow until a clog forms. The ensemble of clogged configurations that had a grain depth of at least 1.5 times the hopper width, W (details in [18]), are subjected to vibrations to unclog the flow. The inclined walls at the base are displaced vertically at a fixed frequency $f = 10\ (g/d_1)^{1/2}$, and varying amplitudes $A = 1\text{–}5 \times 10^{-3}\ d_1$. The vibration strength is characterized by the maximum acceleration, $\Gamma = 4\pi^2 f^2 A$ that

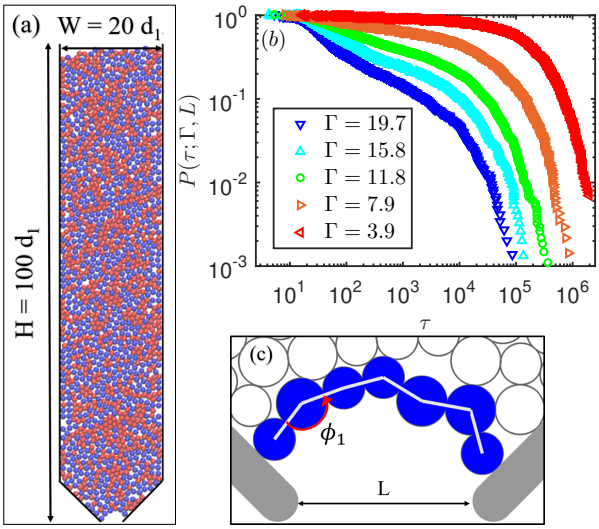

FIG. 1: (color online) (a) Hopper geometry with width $W = 20$, height $H = 100$ filled with a bidisperse mixture of ~ 1600 spherical grains. (b) Complementary cumulative distribution function $P(\tau; \Gamma, L)$ of the unclogging times for opening size $L = 4.2$ and varying vibration amplitudes Γ. (c) Sample five-angle arch with a single opening angle ϕ_1 marked. The lower walls are formed from static, overlapping grains of size d_1, angled at 45°.

falls in the range of $\Gamma = 3.9$–19.7 in units of the gravitational acceleration g. All times are measured in units of the vibration period $T_{vib} = f^{-1}$, and lengths are measured in units of d_1, the small grain diameter. The initiation of flow is observed to be caused by arch failures except in rare cases where the entire arch slides out through the opening before collapsing. The unclogging time, τ, defined as the time between the start of the vibrations to the first time the center of any grain exits the outlet, is measured for each arch, and used to estimate the probability distribution function (PDF), $p(t;\Gamma,L)$, and the complementary cumulative distribution function (CCDF), $P(\tau;\Gamma,L) = \int_\tau^\infty p(t;\Gamma,L)dt$ [19]. The distributions are constructed from ensembles with $N = 1744, 1389, 2718, 1506,$ and 1469 different arches for $\Gamma = 3.9, 7.9, 11.8, 15.8, 19.7$, respectively.

As shown in Fig. 1(b), $P(\tau;\Gamma,4.2)$ reveals broad distributions of unclogging times that show a distinct trend even over the limited range of driving amplitudes studied. As observed in experiments [2], $P(\tau;\Gamma,4.2)$ becomes broader as Γ is reduced, and the mean unclogging time grows from $\langle t\rangle = 1.58\times10^3$ ($\Gamma = 19.7$) to $\langle t\rangle = 2.5\times10^5$ ($\Gamma = 3.9$). The shape of $P(\tau;\Gamma,4.2)$ is characterized by three distinct regions: (i) a fast decay due to arches that break quickly, (ii) a slower decay characterized by a plateau extending over several decades, and (iii) a final fast decay. For the smallest amplitude, $\Gamma = 3.9$, 11 of 1744 arches remained clogged for longer than the maximum simulation time used $T_{sim} = 2\times10^6$, and the shape of $P(\tau;\Gamma,4.2)$ can only be estimated up to T_{sim}. For all other Γ, the simulation time was sufficient to break all the arches. Unlike the experiments [2], we observe a finite cutoff time in these distributions. We investigate the dynamics of the clogging arch at $L = 4.2$ to understand the origin of the broad distributions of τ and their evolution with Γ. For the hopper geometry used, $P(\tau;\Gamma,L)$ shows only a weak dependence on L. [18]

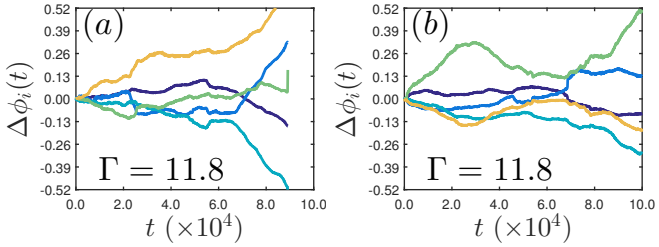

FIG. 2: (color online) Time series of changes $\Delta\phi_i(t)$ (in radians, relative to the initial opening angle $\phi_i(0)$) to the opening angles for two distinct five-angle arches ($N_\phi = 5$) unclogged using the same vibration amplitude $\Gamma = 11.8$. The unclogging times are $t = 89,107$ (a) and $t > 100,000$ (b). The different angles within the arch (different colors within a panel) show correlated evolution in time. The arches undergo a series of reconfigurations, with changes to the angles as large as $30^\circ = 0.52$ *rad*.

Arch Shape Dynamics The clogging arch is identified as the lowest chain of N_g grains spanning the distance between the outlet walls. The shape of the arch is parameterized by $N_\phi = N_g - 2$ opening angles $\phi_i(t)$ (Fig. 1c). At $L = 4.2$, arches with $N_\phi = 3, 4,$ and 5 dominated the ensemble [18]. In response to vibrations, multiple $\phi_i(t)$ reconfigure simultaneously to change the shape of the arch (Fig. 2, and [18]). Reconfigurations of arch shape are characterized by bursts of large changes interspersed with interludes of relatively small changes. Fig. 2 shows that there are large variations in the dynamics from arch to arch. To study the dynamics, we characterize the arch shape by the N_ϕ dimensional vector of opening angles $|\phi(t)\rangle = (\phi_1(t), .., \phi_{N_\phi}(t))$. Since a large enough deformation of the arch should always break it, we expect that the phase space of stable arch shapes has a finite size. A wide range of stable arch shapes are observed, including cases with grains hanging below their neighbors, *i.e.*, $\phi_i > 180^\circ$, which suggests the stability boundary in this space has a complicated shape.

TAMSD and Ergodicity Breaking At a given (Γ, L), we construct an ensemble of arches with a given, fixed number of grains, and treat them as random walkers at "positions" $|\phi(t)\rangle$. The distribution of unclogging times is given by the distribution of first-passage times to a boundary of stability in this space.

The time-averaged mean-squared displacement (TAMSD)[20–23] for each arch is defined as:

$$\delta^2(\Delta,T) = \frac{1}{T-\Delta}\int_0^{T-\Delta}\langle\delta\phi(t,\Delta)|\delta\phi(t,\Delta)\rangle dt, \qquad (1)$$

where $|\delta\phi(t,\Delta)\rangle \equiv |\phi(t+\Delta)\rangle - |\phi(t)\rangle$ is the displacement vector, Δ the lag time, and T the total time elapsed since the initiation of vibration. The ensemble-averaged mean-squared displacement (MSD), without any time averaging, is calculated as $\langle\phi^2(t)\rangle = \frac{1}{N(t)}\sum_{m=1}^{m=N(t)}\langle\phi(t)-\phi(0)|\phi(t)-\phi(0)\rangle_m$, where the index m indicates individual arches [18]. Properties of the stochastic process can be inferred from the ensemble-averaged TAMSD, $\langle\delta^2(\Delta,T)\rangle$, and the MSD.

For a simple random walk, the $\delta^2(\Delta,T)$ are narrowly distributed around their mean $\langle\delta^2(\Delta,T)\rangle$. Consequently, the TAMSD for a single walker approaches the ensemble-averaged MSD: $\lim_{T\to\infty}\delta^2(\Delta,T\to\infty) = \langle\phi^2(t=\Delta)\rangle$, which grows linearly with time. In a CTRW, the TAMSD are random variables [21, 24, 25]. For a waiting time distribution $\lim_{t\to\infty}\psi(t)\sim t^{-1-\alpha}$, with $0<\alpha<1$, CTRWs break ergodicity: $\langle\delta^2(\Delta,T)\rangle$ differs from MSD [21, 24]. In addition, $\langle\phi^2(t)\rangle$ is found to be sub-diffusive with an anomalous exponent α: $\langle\phi^2(t)\rangle\propto t^\alpha$ [25], but $\langle\delta^2(\Delta,T)\rangle$ is diffusive in Δ, with the scaling form $\langle\delta^2(\Delta,T)\rangle\sim\frac{\Delta}{T^{1-\alpha}}$ ($\Delta << T$) [21, 24–26]. In our case, analysis of $|\phi(t)\rangle$ shows a sub-diffusive MSD [18] and diffusive or slightly super-diffusive growth of $\langle\delta^2(\Delta,T)\rangle$ (Fig. 3), suggesting a CTRW description for the arch dynamics. The waiting

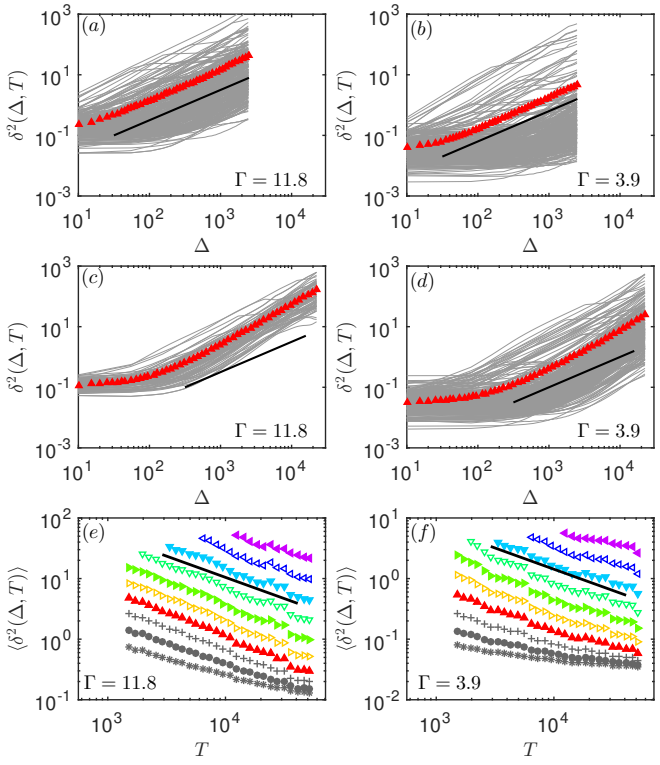

FIG. 3: (color online) (a), (b), (c), (d): Time-averaged mean-squared displacements (TAMSD), $\delta^2(\Delta,T)$ and their ensemble average, $\langle\delta^2(\Delta,T)\rangle$ (▲) shown for two sets of five-angle arches unclogged with vibration amplitudes $\Gamma = 11.8$ (left) and $\Gamma = 3.9$ (right). We contrast ensembles for an intermediate and a long total averaging time, $T = 5\times10^3$ (a), (b) and $T = 4.5\times10^4$ (c), (d). All arches that survive for times $\geq T$ are included. The black lines show a linear slope $\sim\Delta$, as expected for a subdiffusive CTRW with a power law waiting time distribution. (e), (f): Scaling of $\langle\delta^2(\Delta,T)\rangle$ for both sets of arches. The different symbols show $\langle\delta^2(\Delta,T)\rangle$ evaluated for fixed values of the lag time $\Delta = 24$ (∗), $\Delta = 44$ (•), $\Delta = 81$ (+), $\Delta = 149$ (▲), $\Delta = 272$ (▷), $\Delta = 496$ (▶), $\Delta = 904$ (▽), $\Delta = 1649$ (▼), $\Delta = 3007$ (◁), $\Delta = 5,484$ (◀). The black line indicates a T dependence $\sim T^{-0.7=-1+0.3}$.

times in the CTRW are the times between significant reconfigurations of the arch shapes. We infer the form of $\psi(t)$ from TAMSD and MSD measurements.

Fig. 3 shows $\delta^2(\Delta,T)$, and the ensemble average, $\langle\delta^2(\Delta,T)\rangle$, for two different ensembles with $N_\phi = 5$ at $\Gamma = 11.8$ and $\Gamma = 3.9$. These amplitudes were chosen because their $p(t;\Gamma,L)$ differ significantly. In addition, there are a sufficient number of long-lived arches to provide adequate statistics for time and ensemble averaging [18]. For $T = 5000$, there is a broad scatter in $\delta^2(\Delta,T)$ around $\langle\delta^2(\Delta,T)\rangle$ at both values of Γ. This broad scatter is a signature of ergodicity breaking [21, 22, 27]. Some details in the TAMSD behavior differ from the known features of an ideal CTRW. For the longer averaging time $T = 45000$, the broad scatter is still present at $\Gamma = 3.9$, but there is narrowing at $\Gamma = 11.8$, which hints at a possible recovery of ergodicity. In addition, the Δ scaling of $\langle\delta^2(\Delta,T)\rangle$ emerges only for $\Delta > \Delta_0 \approx 10^2$, indicating a short-time cutoff in the the waiting time distribution. Finally, for both amplitudes, the TAMSD shows a superdiffusive slope in Δ at long T. These details indicate ways in which the arch dynamics differ from those of an ideal CTRW. As we show below, the differences are heightened in the first-passage process, and some can be reconciled within a CTRW model by changing the form of $\psi(t)$ from a pure power law to an even broader distribution.

Effects of changing Γ Figs. 3 (e) and (f) illustrate the T dependence of $\langle\delta^2(\Delta,T)\rangle$ for five-angle arches at $\Gamma = 11.8$ and $\Gamma = 3.9$, over a range of Δ. The predicted scaling form, $\langle\delta^2(\Delta,T)\rangle \sim \frac{\Delta}{T^{1-\alpha}}$, is obeyed for $\Delta_0 < \Delta << T$. Within statistical errors, $\alpha \simeq 0.3$ for both values of Γ. However, $\langle\delta^2(\Delta,T)\rangle$ shows a change in magnitude of ≈ 10, which corresponds to a decrease in the effective diffusion coefficient D_α as the vibration amplitude is decreased from $\Gamma = 11.8$ to 3.9. The same reduction in magnitude is observed in $\langle\phi^2(t)\rangle$ [18].

In a CTRW, the properties of the random variable, $\delta^2(\Delta,T)$, are characterized by the distribution $\phi(\xi)$ of the scaled quantity $\xi(\Delta,T) = \delta^2(\Delta,T)/\langle\delta^2(\Delta,T)\rangle$. For a pure random walk, this distribution approaches a delta function $\delta(\xi-1)$ at large T. In contrast, for a CTRW with a power law distribution of waiting times, $\phi(\xi)$ approaches a universal form parametrized by the anomalous exponent α at large Δ and T [24]. $\phi(\xi)$ is a more sensitive probe of the stochastic dynamics than $\langle\delta^2(\Delta,T)\rangle$. In particular, the variance EB $\equiv \langle\xi^2\rangle - \langle\xi\rangle^2$ provides a *quantitative* measure of ergodicity breaking [24]. Measurements of $\phi(\xi)$ for the same ensembles of arches used in the TAMSD analysis are shown in Fig. 4. We find that $\phi(\xi)$ depends only on the ratio Δ/T over a broad range of Δ and T [18]. We therefore compute $\phi(\xi)$, and EB as a function of Δ/T, by averaging over different values of Δ and T. For $\Delta/T = 0.1$–0.4, the results are roughly independent of Δ/T. In this regime, EB is a sensitive function of Γ, with values of 40 (6) at $\Gamma = 11.8$ (3.9). Both values are much larger than the asymptotic prediction, $EB = 0.8$, for the pure power law $\psi(t) \simeq t^{-1-\alpha}$ with $\alpha = 0.3$ [24]. Fig 5 demonstrates that the distributions of unclogging times $p(t;\Gamma,L)$, which correspond to first passage times, are also broader than expected from a power law CTRW with $\psi(t) \propto t^{-1-\alpha}$, $\alpha = 0.3$, and develop extended plateaus as Γ decreases. These results suggest that the waiting time distribution $\psi(t)$ is itself becoming broader as the vibration amplitude decreases even though the TAMSD measurements are consistent with $\alpha = 0.3$, independent of Γ. We report below on the first-passage properties of one particular model of $\psi(t)$ that reconciles the TAMSD and these $p(t;\Gamma,L)$ results.

First Passage Time Simulations We performed numerical simulations to compute the first-passage-time distribution for a broadened waiting time distribution $\psi(t) \propto (\frac{\alpha}{at})(\alpha ln(t))^{1/a-1}e^{-(\alpha ln(t))^{1/a}}e^{-\lambda t}$, with $a \geq 1$,

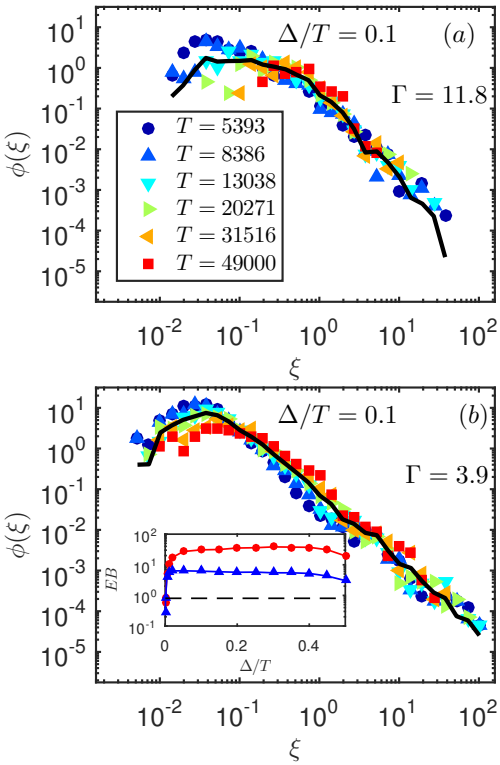

FIG. 4: (color online) Distributions $\phi(\xi)$ of the normalized TAMSD $\xi = \frac{\delta^2}{\langle\delta^2\rangle}$ for $\Gamma = 11.8$ (a) and $\Gamma = 3.9$ (b). The shapes of the distributions, shown here for $\Delta/T = 0.1$ and the different T values in the legend, depend on the ratio Δ/T. The averaged $\phi(\xi)$, black solid line, is used to compute the EB at $\Delta/T = 0.1$. Inset to (b): the EB parameter, $\langle\xi^2\rangle - \langle\xi\rangle^2$ for amplitudes $\Gamma = 3.9$ (•) and $\Gamma = 11.8$ (▲) as a function of Δ/T, computed using averaged $\phi(\xi)$ over a range of Δ/T [18], is roughly constant in the range $\Delta/T = 0.1$–0.4. The dashed black line indicates the expected EB value for a power law $\psi(t)$ with $\alpha = 0.3$.

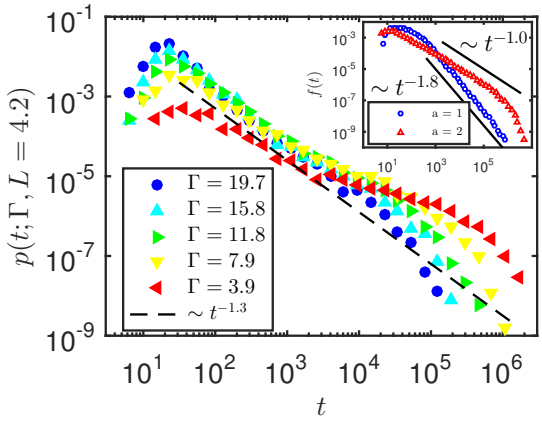

FIG. 5: (color online) Probability distribution functions $p(t;\Gamma, L)$ for the unclogging times measured for varying vibration strengths Γ. These distributions are seen to have a peak at short times followed by a broad, slow decay, and an upper cutoff time at long times. Inset: Examples of numerical first passage time distributions $f(t)$ for a finite 1d interval, see SI material [18]. For a pure power law waiting time distribution $\psi(t)$ (inset $a = 1$), the first passage time distribution $f(t)$ has the same power law, but a "stretched" $\psi(t)$ (inset $a = 2$) produces a broader tail in $f(t)$. Solid lines are included as guides for the eye.

which asymptotes to $\sim t^{-1-\alpha}e^{-\lambda t}$ for $a = 1$. This distribution, which can be derived from a trap model with a stretched exponential distribution of barriers, becomes increasingly heavy-tailed as a is increased. A stretched exponential distribution of barriers has been shown to be consistent with experimental results on unclogging [16]. The effect of increasing a is reasonably approximated by a power law with exponent, $\alpha_{\rm eff}(a)$ that appears smaller than the nominal α [18].

For simplicity, we investigate the process on a finite 1d lattice [18]. As expected [28, 29], the first passage time distribution $f(t)$ decays asymptotically as $\sim t^{-1-\alpha}$ at $a = 1$. In contrast, for $a > 1$, the decay is slower than $\sim t^{-1-\alpha}$, and the asymptotic forms depend on the lattice size and the cutoff time scale $1/\lambda$.

The distributions obtained from this model compare well to the distribution, $p(t;\Gamma, L)$, of unclogging times, and indicate a increasing from 1 to $\simeq 2$ as Γ decreases from 19.7 to 3.9 (Fig. 5). The increasingly slower decay of the distributions is consistent with EB increasing with decreasing Γ. Ensemble averaged measurements such as the TAMSD (Fig. 3) are not sensitive to the precise form of the asymptotic decay of $\psi(t)$ [18], and therefore, cannot provide information about the changing dynamics with Γ.

Discussion We have presented a detailed analysis of the dynamics of arches leading to collapse in simulations of vibrated hoppers. The physical picture that emerges is that, in response to vibrations, arches evolve in a landscape of locally stable shapes reminiscent of trap models [14] with an anomalously broad distribution of trap depths. The random environment created by the grains above the arch, including weak and strong force-bearing networks [9, 30] presumably leads to this large variability. Vibrations induce changes in the shape of the arches, which can be modeled as an activated escape from a trap; a locally stable shape. The exploration of this landscape of shapes leads to a broad distribution of unclogging times, which is, therefore, a direct reflection of the disordered nature of clogged states.

Our simulations show that the distribution of unclogging times is sensitive to the details of the landscape explored by the arches. The CTRW model we propose is the simplest stochastic model that captures the dynamics of the arches in our simulations. It is possible that a more sophisticated model such as one in which the waiting time depends on the arch shape would provide a better description of arch failure. In addition to providing a physical picture of the dynamics, our work shows that the

CTRW or trap-model paradigm provides a useful interpretive framework for analyzing experiments on unclogging and provides an important tool for devising methods to unclog flows.

Acknowledgements: The work of CM and BC has been supported by NSF-DMR 1409093 as well as the Brandeis IGERT program. SKB thanks Narayanan Menon and Rama Govindarajan for their support, and acknowledges funding from TCIS Hyderabad, ICTS Bangalore, the APS-IUSSTF for a travel grant and NSF-DMR 120778 and NSF-DMR 1506750 at UMass Amherst. We would like to thank Iker Zuriguel, Ángel Garcimartín, Aparna Baskaran, and Kabir Ramola for helpful discussions and comments.

* cbrady@brandeis.edu

[1] I. Zuriguel, D. R. Parisi, R. C. Hidalgo, C. Lozano, A. Janda, P. A. Gago, J. P. Peralta, L. M. Ferrer, L. A. Pugnaloni, E. Clément, D. Maza, I. Pagonabarraga, and A. Garcimartín, Sci. Rep. **4** (2014).
[2] C. Lozano, I. Zuriguel, and A. Garcimartín, Phys. Rev. E **91** (2015).
[3] I. Zuriguel, Pap. Phys. **6**, 13 (2014).
[4] D. Helbing, I. Farkas, and T. Vicsek, Nature **407**, 487 (2000).
[5] C. E. Thomas and D. E. Durian, Phys. Rev. Lett. **114**, 1 (2015).
[6] K. To, P. Y. Lai, and H. K. Pak, Phys. Rev. Lett. **86**, 71 (2001).
[7] I. Zuriguel, A. Garcimartín, D. Maza, L. A. Pugnaloni, J. M. Pastor, and L. Plata, Phys. Rev. E - Stat. Nonlinear, Soft Matter Phys. **71**, 1 (2005).
[8] A. Janda, I. Zuriguel, A. Garcimartín, L. A. Pugnaloni, and D. Maza, EPL Europhys. Lett. **84**, 44002 (2008).
[9] J. Tang, S. Sagdiphour, R. Behringer, M. Nakagawa, and S. Luding, in *AIP Conference Proceedings*, Vol. 1145 (AIP, 2009) pp. 515–518.
[10] L. Kondic, Granul. Matter **16**, 235 (2014).
[11] A. Janda, D. Maza, A. Garcimartin, E. Kolb, J. Lanuza, and E. Clement, EPL Europhys. Lett. **87**, 24002 (2009).
[12] C. Mankoc, A. Garcimartín, I. Zuriguel, D. Maza, and L. A. Pugnaloni, Phys. Rev. E **80** (2009).
[13] R. Metzler, J.-H. Jeon, A. G. Cherstvy, and E. Barkai, Phys. Chem. Chem. Phys. **16**, 24128 (2014).
[14] C. Monthus and J.-P. Bouchaud, J. Phys. A. Math. Gen. **29**, 3847 (1996).
[15] S. Redner, *A Guide to First-Passage Processes*, A Guide to First-passage Processes (Cambridge University Press, 2001).
[16] A. Nicolas, A. Garcimartín, and I. Zuriguel, (2017), arXiv:1711.04455.
[17] S. Plimpton, J. Comput. Phys. **117**, 1 (1995); Http://lammps.sandia.gov.
[18] See supplementary material at [URL will be inserted by publisher] for details of the molecular dynamics simulations, examples of the arch angle time series, ensemble MSD measurements, and details of the model first-passage time computations.
[19] M. E. Newman, Contemp. Phys. **46**, 323 (2005).
[20] I. Golding and E. C. Cox, Phys. Rev. Lett. **96** (2006).
[21] A. Lubelski, I. M. Sokolov, and J. Klafter, Phys. Rev. Lett. **100** (2008).
[22] J.-H. Jeon and R. Metzler, J. Phys. A Math. Theor. **43** (2010).
[23] S. M. Tabei, S. Burov, H. Y. Kim, A. Kuznetsov, T. Huynh, J. Jureller, L. H. Philipson, A. R. Dinner, and N. F. Scherer, Proc Natl Acad Sci U S A **110**, 4911 (2013).
[24] Y. He, S. Burov, R. Metzler, and E. Barkai, Phys. Rev. Lett. **101** (2008).
[25] J. Klafter and I. Sokolov, *First Steps in Random Walks: From Tools to Applications* (OUP Oxford, 2011).
[26] T. Miyaguchi and T. Akimoto, Phys. Rev. E - Stat. Nonlinear, Soft Matter Phys. **83** (2011); **87** (2013).
[27] J. Bewerunge, I. Ladadwa, F. Platten, C. Zunke, A. Heuer, and S. U. Egelhaaf, Phys. Chem. Chem. Phys. **18**, 18887 (2016).
[28] R. Metzler and J. Klafter, J. Phys. A Math. Gen **37**, 161 (2004).
[29] R. Metzler and J. Klafter, Phys. A Stat. Mech. its Appl. **278**, 107 (2000).
[30] R. C. Hidalgo, C. Lozano, I. Zuriguel, and A. Garcimartin, Granul. Matter **15**, 841 (2013).